

Search for CP violation using T -odd correlations in $D_{(s)}^+ \rightarrow K^+ K^- \pi^+ \pi^0$, $D_{(s)}^+ \rightarrow K^+ \pi^- \pi^+ \pi^0$, and $D^+ \rightarrow K^- \pi^+ \pi^+ \pi^0$ decays

L. K. Li , A. J. Schwartz , E. Won , K. Kinoshita , I. Adachi , H. Aihara , S. Al Said , D. M. Asner , V. Aulchenko , T. Aushev , V. Babu , Sw. Banerjee , P. Behera , K. Belous , J. Bennett , M. Bessner , T. Bilka , D. Biswas , A. Bobrov , D. Bodrov , G. Bonvicini , J. Borah , M. Bračko , P. Branchini , A. Budano , D. Červenkov , M.-C. Chang , B. G. Cheon , H. E. Cho , K. Cho , S.-K. Choi , Y. Choi , S. Choudhury , D. Cinabro , J. Cochran , S. Das , G. De Nardo , G. De Pietro , R. Dhamija , F. Di Capua , J. Dingfelder , Z. Doležal , T. V. Dong , S. Dubey , D. Epifanov , A. Frey , B. G. Fulsom , V. Gaur , A. Giri , P. Goldenzweig , G. Gong , E. Graziani , D. Greenwald , T. Gu , Y. Guan , K. Gudkova , C. Hadjivasiliou , T. Hara , K. Hayasaka , H. Hayashii , D. Herrmann , W.-S. Hou , C.-L. Hsu , N. Ipsita , A. Ishikawa , R. Itoh , M. Iwasaki , W. W. Jacobs , E.-J. Jang , Q. P. Ji , S. Jia , Y. Jin , K. K. Joo , J. Kahn , A. B. Kaliyar , C. Kiesling , C. H. Kim , D. Y. Kim , K.-H. Kim , Y. J. Kim , Y.-K. Kim , H. Kindo , P. Kodyš , A. Korobov , S. Korpar , E. Kovalenko , P. Križan , P. Krokovny , M. Kumar , R. Kumar , K. Kumara , Y.-J. Kwon , Y.-T. Lai , T. Lam , S. C. Lee , Y. Li , J. Libby , K. Lieret , Y.-R. Lin , D. Liventsev , Y. Ma , M. Masuda , T. Matsuda , D. Matvienko , S. K. Maurya , F. Meier , M. Merola , F. Metzner , R. Mizuk , G. B. Mohanty , M. Nakao , D. Narwal , Z. Natkaniec , A. Natchii , L. Nayak , N. K. Nisar , S. Nishida , S. Ogawa , H. Ono , P. Oskin , G. Pakhlova , S. Pardi , H. Park , J. Park , S.-H. Park , A. Passeri , S. Patra , S. Paul , R. Pestotnik , L. E. Piilonen , T. Podobnik , E. Prencipe , M. T. Prim , G. Russo , S. Sandilya , A. Sangal , L. Santelj , V. Savinov , G. Schnell , C. Schwanda , Y. Seino , M. E. Sevir , W. Shan , M. Shapkin , C. Sharma , J.-G. Shiu , B. Shwartz , E. Solovieva , M. Starič , Z. S. Stottler , M. Sumihama , M. Takizawa , K. Tanida , F. Tenchini , M. Uchida , T. Uglov , Y. Unno , K. Uno , S. Uno , G. Varner , K. E. Varvell , A. Vinokurova , D. Wang , E. Wang , X. L. Wang , S. Watanuki , O. Werbycka , X. Xu , B. D. Yabsley , W. Yan , S. B. Yang , J. H. Yin , Y. Yook , Z. P. Zhang , V. Zhilich , and V. Zhukova 

(The Belle Collaboration)

We search for CP violation using T -odd correlations in five $D_{(s)}^+$ and $D_{(s)}^-$ four-body decays. Our analysis is based on 980 fb^{-1} of data collected by the Belle detector at the KEKB energy-asymmetric e^+e^- collider. Our results for the T -odd CP -violating parameter $a_{CP}^{T\text{-odd}}$ are: $a_{CP}^{T\text{-odd}}(D^+ \rightarrow K^- K^+ \pi^+ \pi^0) = (+2.6 \pm 6.6 \pm 1.3) \times 10^{-3}$, $a_{CP}^{T\text{-odd}}(D^+ \rightarrow K^+ \pi^- \pi^+ \pi^0) = (-1.3 \pm 4.2 \pm 0.1) \times 10^{-2}$, $a_{CP}^{T\text{-odd}}(D^+ \rightarrow K^- \pi^+ \pi^+ \pi^0) = (+0.2 \pm 1.5 \pm 0.8) \times 10^{-3}$, $a_{CP}^{T\text{-odd}}(D_s^+ \rightarrow K^+ \pi^- \pi^+ \pi^0) = (-1.1 \pm 2.2 \pm 0.1) \times 10^{-2}$, and $a_{CP}^{T\text{-odd}}(D_s^+ \rightarrow K^- K^+ \pi^+ \pi^0) = (+2.2 \pm 3.3 \pm 4.3) \times 10^{-3}$, where the uncertainties are statistical and systematic, respectively. These results are the first such measurements and are all consistent with zero. They include the first measurement for a D_s^+ singly Cabibbo-suppressed decay, and the first measurement for a D meson doubly Cabibbo-suppressed decay. We also measure $a_{CP}^{T\text{-odd}}$ in different subregions of phase space, where the decays are dominated by different intermediate resonance states such as $D^+ \rightarrow \phi \rho^+$, $\bar{K}^{*0} K^{*+}$, and $\bar{K}^{*0} \rho^+$; and $D_s^+ \rightarrow K^{*+} \rho^0$, $K^{*0} \rho^+$, $\phi \rho^+$, and $\bar{K}^{*0} K^{*+}$. No evidence for CP violation is found.

I. INTRODUCTION

CP violation is required to explain the matter-antimatter asymmetry of the Universe [1]. In the Standard Model (SM), CP violation arises naturally due to the presence of a complex phase in the Cabibbo-Kobayashi-Maskawa (CKM) matrix [2, 3]. However, this source is insufficient to explain the absence of antimatter in the Universe. Thus it is important to search for new sources of CP violation beyond the SM. CP violation in charm decays is predicted to be very small, $\lesssim 10^{-3}$ [4–6], and observing it significantly above this level would imply physics beyond the SM [7]. Charm decays proceeding via singly Cabibbo-suppressed (SCS) amplitudes are es-

pecially promising for such searches, as these amplitudes can have internal loops containing new mediators or couplings [4]. To date, the only observation of CP violation in charm decays has been reported in the SCS decays $D^0 \rightarrow K^+ K^-$ and $D^0 \rightarrow \pi^+ \pi^-$ [8]. In this paper, we present the first search for CP violation in several additional Cabibbo-suppressed decay channels.

We study four-body decays $D_{(s)}^+ \rightarrow P_1 P_2 P_3 P_4$, where P corresponds to a pseudoscalar meson, by measuring the triple product of the momenta of three of the four final-state particles: $C_T \equiv \vec{p}_1 \cdot (\vec{p}_2 \times \vec{p}_3)$. These momenta are evaluated in the $D_{(s)}^+$ rest frame. We define an analogous observable \bar{C}_T for charge-conjugate $D_{(s)}^-$ decays. These observables are T odd, i.e., they change sign under time-

reversal. Thus, if the distribution of C_T is asymmetric about zero, this could indicate T violation. To quantify such an asymmetry, we define the variables

$$A_T \equiv \frac{N(C_T > 0) - N(C_T < 0)}{N(C_T > 0) + N(C_T < 0)}, \quad (1)$$

$$\bar{A}_T \equiv \frac{\bar{N}(-\bar{C}_T > 0) - \bar{N}(-\bar{C}_T < 0)}{\bar{N}(-\bar{C}_T > 0) + \bar{N}(-\bar{C}_T < 0)}, \quad (2)$$

where N and \bar{N} are the yields of $D_{(s)}^+$ and $D_{(s)}^-$ decays, respectively. The minus signs included in the definition of \bar{A}_T correspond to a parity transformation; in this manner A_T and \bar{A}_T are CP -conjugate quantities. However, final-state interactions (FSI) can also give rise to nonzero A_T or \bar{A}_T and thus mimic T violation. To isolate T violation, we measure the difference

$$a_{CP}^{T\text{-odd}} \equiv \frac{1}{2}(A_T - \bar{A}_T), \quad (3)$$

in which asymmetries arising from FSI cancel. In addition to being T -violating, $a_{CP}^{T\text{-odd}} \neq 0$ is manifestly CP -violating. The amount of CP violation is proportional to $\sin \phi \cos \delta$, where ϕ and δ are the weak and strong phase differences, respectively, between at least two amplitudes contributing to the decay [9]. This is in contrast to a CP asymmetry in D and \bar{D} partial widths, \mathcal{A}_{CP} , which is proportional to $\sin \phi \sin \delta$. If the strong phase difference δ is small, $\mathcal{A}_{CP} \approx 0$ but $a_{CP}^{T\text{-odd}}$ could significantly differ from zero.

Experimentally, $a_{CP}^{T\text{-odd}}$ has been measured for several D decay modes [10–16]. These measurements include two results for charged D mesons: $a_{CP}^{T\text{-odd}}(D^+ \rightarrow K_s^0 K^+ \pi^+ \pi^-) = (-1.10 \pm 1.09)\%$ [10] and $a_{CP}^{T\text{-odd}}(D_s^+ \rightarrow K_s^0 K^+ \pi^+ \pi^-) = (-1.39 \pm 0.84)\%$ [11]. Here we measure $a_{CP}^{T\text{-odd}}$ for five additional $D_{(s)}^+$ decays: $D_{(s)}^+ \rightarrow K^+ K^- \pi^+ \pi^0$, $D_{(s)}^+ \rightarrow K^+ \pi^- \pi^+ \pi^0$, and $D^+ \rightarrow K^- \pi^+ \pi^+ \pi^0$. The first D^+ decay and the second D_s^+ decay are SCS; the second D^+ decay is doubly Cabibbo-suppressed (DCS); and the first D_s^+ decay and last D^+ decay are Cabibbo-favored (CF). These are the first such measurements, and we also perform them in seven subregions of phase space. In these different subregions, the decays proceed predominantly via intermediate processes such as $D^+ \rightarrow \phi \rho^+$, $\bar{K}^{*0} K^{*+}$, and $\bar{K}^{*0} \rho^+$; and $D_s^+ \rightarrow K^{*+} \rho^0$, $K^{*0} \rho^+$, $\phi \rho^+$, and $\bar{K}^{*0} K^{*+}$. As the intermediate states give rise to different strong phase differences δ [17], the subregions can have different values of $a_{CP}^{T\text{-odd}}$.

II. BELLE DETECTOR AND DATA SETS

This measurement is based on the full data set of the Belle experiment, which corresponds to an integrated luminosity of 980 fb^{-1} collected at or near the $\Upsilon(nS)$ ($n = 1, 2, 3, 4, 5$) resonances. The Belle experiment ran

at the KEKB energy-asymmetric collider [18]. The Belle detector is a large-solid-angle magnetic spectrometer consisting of a silicon vertex detector (SVD), a 50-layer central drift chamber (CDC), an array of aerogel threshold Cherenkov counters (ACC), a barrel-like arrangement of time-of-flight scintillation counters (TOF), and an electromagnetic calorimeter (ECL) comprising CsI(Tl) crystals located inside a superconducting solenoid coil providing a 1.5 T magnetic field. An iron flux return yoke located outside the coil is instrumented to detect K_L^0 mesons and to identify muons (KLM). A detailed description of the detector is given in Ref. [19].

Monte Carlo (MC) simulated events are generated from e^+e^- collisions based on PYTHIA [20] and EVTGEN [21]. All particles are propagated through a full detector simulation using GEANT3 [22]. Final-state radiation from charged particles is simulated using PHOTOS [23]. The MC samples include $e^+e^- \rightarrow q\bar{q}$ ($q = u, d, s, c$) and $e^+e^- \rightarrow B\bar{B}$ events, and $e^+e^- \rightarrow B_{(s)}^{(*)}\bar{B}_{(s)}^{(*)}X$ events produced at the $\Upsilon(5S)$ resonance. These MC samples correspond to an integrated luminosity three times that of the data, and they are used to optimize event selection criteria, study backgrounds, and evaluate systematic uncertainties.

III. EVENT SELECTION

We reconstruct D^+ decays into three final states, $K^+K^-\pi^+\pi^0$, $K^-\pi^+\pi^+\pi^0$, and $K^+\pi^-\pi^+\pi^0$; and D_s^+ decays into two final states, $K^+\pi^-\pi^+\pi^0$ and $K^-K^+\pi^+\pi^0$. The selection criteria for the Cabibbo-suppressed decays are the same as those used to measure their branching fractions in Ref. [24]. The criteria for the CF decays are separately optimized for the A_T measurement presented here. Charged tracks are reconstructed in the CDC and SVD [19]. To ensure that tracks are well reconstructed, each final-state charged particle is required to have at least two SVD hits in each of the longitudinal and azimuthal measuring coordinates. We identify K^\pm and π^\pm candidates based on particle-identification likelihoods calculated for different particle hypotheses, \mathcal{L}_i ($i = \pi, K$). These likelihoods are calculated based on information from the ACC, CDC, and TOF [25]. Tracks with $\mathcal{L}_K/(\mathcal{L}_K + \mathcal{L}_\pi) > 0.6$ are identified as kaons; otherwise, tracks are considered as pions. To suppress background from $D_{(s)}^+$ semileptonic decays, tracks that are highly electron-like [$\mathcal{L}_e/(\mathcal{L}_e + \mathcal{L}_{\text{hadron}}) > 0.95$] or muon-like [$\mathcal{L}_\mu/(\mathcal{L}_\mu + \mathcal{L}_\pi + \mathcal{L}_K) > 0.95$] are rejected, where these likelihoods are calculated based on information mainly from the ECL and KLM, respectively [26, 27]. These requirements have overall efficiencies of about 90% for kaons and 95% for pions.

We reconstruct π^0 candidates from pairs of photons. Photon candidates are identified from energy clusters in

the ECL that are not associated with any charged track. The photon energy is required to be greater than 50 MeV if reconstructed in the barrel region (covering the polar angle $32^\circ < \theta < 129^\circ$), and greater than 100 MeV if reconstructed in the endcap regions ($12^\circ < \theta < 31^\circ$ or $132^\circ < \theta < 157^\circ$). The energy deposited in the 3×3 array of crystals centered on the crystal with the highest energy is compared to the energy deposited in the corresponding 5×5 array of crystals; the ratio of the first energy to the second is required to be greater than 0.80. Candidate $\pi^0 \rightarrow \gamma\gamma$ decays are reconstructed from photon pairs having an invariant mass satisfying $115 \text{ MeV}/c^2 < M(\gamma\gamma) < 150 \text{ MeV}/c^2$; this region corresponds to about three standard deviations (σ) in $M(\gamma\gamma)$ resolution. The π^0 momentum is required to be greater than 0.40 GeV/ c . To suppress backgrounds such as $D_{(s)}^+ \rightarrow K^+ K_s^0 \pi^0$, we veto candidates in which a final-state $\pi^+ \pi^-$ pair has an invariant mass within $10 \text{ MeV}/c^2$ (3σ) of the K_s^0 mass [28].

A $D_{(s)}^+$ candidate is reconstructed by combining $K^- K^+ \pi^+$ or $K^\pm \pi^\mp \pi^+$ track combinations with a π^0 candidate. A vertex fit is performed for the three charged tracks, and the resulting fit quality is defined as χ_{vtx}^2 . The coordinates of the fitted vertex are assigned as the $D_{(s)}^+$ decay vertex position. The momenta of the two photons from the π^0 candidate are then fit to this vertex position, with the invariant mass constrained to the nominal π^0 mass [28]; the resulting fit quality ($\chi_{\pi^0}^2$) is required to satisfy $\chi_{\pi^0}^2 < 8$. The $D_{(s)}^+$ production vertex is determined by fitting the $D_{(s)}^+$ trajectory to the e^+e^- interaction point (IP), which is determined from the beam profiles. This vertex fit quality is defined as χ_{IP}^2 .

We calculate the significance of the $D_{(s)}^+$ decay length L/σ_L , where L is the projection of the vector running from the production vertex to the $D_{(s)}^+$ decay vertex onto the momentum direction. The corresponding uncertainty σ_L is calculated by propagating uncertainties in the vertices and the $D_{(s)}^+$ momentum, including their correlations. We subsequently require $\chi_{\text{vtx}}^2 + \chi_{\text{IP}}^2 < 14$ and $L/\sigma_L > 4$ for $D^+ \rightarrow K^- K^+ \pi^+ \pi^0$ decays; $\chi_{\text{vtx}}^2 + \chi_{\text{IP}}^2 < 10$ and $L/\sigma_L > 9$ for $D^+ \rightarrow K^+ \pi^- \pi^+ \pi^0$ decays; $\chi_{\text{vtx}}^2 + \chi_{\text{IP}}^2 < 10$ and $L/\sigma_L > 2.5$ for $D_s^+ \rightarrow K^+ \pi^- \pi^+ \pi^0$ decays; $\chi_{\text{vtx}}^2 + \chi_{\text{IP}}^2 < 17$ and $L/\sigma_L > 3$ for $D^+ \rightarrow K^- \pi^+ \pi^+ \pi^0$ decays; and $\chi_{\text{vtx}}^2 + \chi_{\text{IP}}^2 < 20$ and $L/\sigma_L > 1$ for $D_s^+ \rightarrow K^- K^+ \pi^+ \pi^0$ decays. These criteria are obtained by maximizing a figure-of-merit, $S/\sqrt{S+B}$, where S and B are the numbers of signal and background events expected in a signal region $-30 \text{ MeV}/c^2 < (M(D) - m_D) < 20 \text{ MeV}/c^2$. Here, $M(D)$ is the invariant mass of a reconstructed D^+ or D_s^+ candidate, and m_D is the known D^+ or D_s^+ mass [28]. This region corresponds to $\pm 2.5\sigma$ in resolution. To reduce combinatorial backgrounds fur-

ther, the $D_{(s)}^+$ momentum in the e^+e^- center-of-mass frame is required to be greater than 2.9 GeV/ c for $D_s^+ \rightarrow K^+ \pi^- \pi^+ \pi^0$ decays, and greater than 2.5 GeV/ c for the other decay modes.

After applying all selection criteria, about 10% of events for D^+ decay modes and 15% of events for D_s^+ decay modes have multiple signal candidates. For these events, the average multiplicity is about 2.2 candidates per event. Such multiple candidates arise from the large number of low momentum π^\pm tracks and π^0 candidates. We select a single $D_{(s)}^+$ candidate per event by choosing the one with the smallest value of the sum $\chi_{\pi^0}^2 + \chi_{\text{vtx}}^2 + \chi_{\text{IP}}^2$. Based on MC simulation, this criterion selects the correct signal candidate 68% of the time.

We veto several peaking backgrounds arising from D^{*+} decays in which the final-state particles are the same as those for the signal modes. A detailed description of this veto is given in Ref. [24]. The veto requirements reject only 1%-3% of signal decays while reducing the D^{*+} backgrounds to a negligible level.

IV. MEASUREMENT OF $a_{CP}^{T\text{-odd}}$

We extract the signal yields via an extended unbinned maximum-likelihood fit to the $M(D)$ distributions. The probability density function (PDF) used to describe backgrounds is taken to be a third-order polynomial for $D^+ \rightarrow K^- K^+ \pi^+ \pi^0$ and a second-order polynomial for the other decay modes. All parameters of these polynomials are free to vary in the fit.

The PDF used to describe signal decays is taken to be the sum of three asymmetric Gaussian (AG) functions and a Crystal Ball (CB) function [29], all having a common mean parameter μ but with different width parameters σ . An additional term is included to describe final-state radiation (FSR). This term is the sum of a Gaussian function and a CB function. All signal parameters are fixed to MC values. However, the mean parameters of the Gaussian functions have a common shift parameter δ_μ , and the widths have a common scaling parameter k_σ ; these two parameters are floated in the fit to account for differences between MC simulation and data. For the large $D^+ \rightarrow K^- \pi^+ \pi^+ \pi^0$ sample, δ_μ and k_σ are floated separately for D^+ and D^- decays; this improves the fit quality. For the other decay modes, the difference in resolution between $D_{(s)}^+$ and $D_{(s)}^-$ decays is negligible, and we use the same parameters δ_μ and k_σ for both samples. We fit the $M(D)$ distributions of the data to determine δ_μ and k_σ along with parameters of the background PDFs; these are then fixed for subsequent fits.

We define C_T as the triple product of the momenta of three charged final-state particles in the $D_{(s)}^+$ rest frame. For $D^+ \rightarrow K^- K^+ \pi^+ \pi^0$ decays, $C_T = \vec{p}_{K^-} \cdot (\vec{p}_{K^+} \times \vec{p}_{\pi^+})$, and for the charge-conjugate $D^- \rightarrow K^+ K^- \pi^- \pi^0$ decay,

$\bar{C}_T = \vec{p}_{K^+} \cdot (\vec{p}_{K^-} \times \vec{p}_{\pi^-})$. For $D^+ \rightarrow K^- \pi^+ \pi^+ \pi^0$ decays, the same-sign pions are distinguished by their momenta: $C_T = \vec{p}_{K^-} \cdot (\vec{p}_{\pi_h^+} \times \vec{p}_{\pi_l^+})$ for D^+ decays and $\bar{C}_T = \vec{p}_{K^+} \cdot (\vec{p}_{\pi_h^-} \times \vec{p}_{\pi_l^-})$ for D^- decays, where π_h and π_l denote the pions with higher and lower momentum.

We divide the $D_{(s)}^\pm$ candidates into four subsamples based on the $D_{(s)}^\pm$ charge and the sign of C_T or \bar{C}_T : (1) $D_{(s)}^+$ with $C_T > 0$, (2) $D_{(s)}^+$ with $C_T < 0$, (3) $D_{(s)}^-$ with $-\bar{C}_T > 0$, and (4) $D_{(s)}^-$ with $-\bar{C}_T < 0$. Subsamples (1) and (3) are related by a CP transformation, as are subsamples (2) and (4). The asymmetries A_T and \bar{A}_T are defined in terms of these signal yields in Eq. (2), and the T -violating asymmetry $a_{CP}^{T\text{-odd}}$ is defined in terms of A_T and \bar{A}_T in Eq. (3). We fit these four subsamples simultaneously, taking the independent fitted parameters to be $N_{\bar{D}} = N(C_T > 0) + N(C_T < 0)$, $N_{\bar{D}} = \bar{N}(-\bar{C}_T > 0) + \bar{N}(-\bar{C}_T < 0)$, A_T , and $a_{CP}^{T\text{-odd}}$. We test this fitting procedure on MC samples and obtain fitted values for $a_{CP}^{T\text{-odd}}$ always consistent with the input values within their statistical uncertainties. The results of the fits to data are plotted in Fig. 1 and listed in Table I. The plots show good agreement between the data and the fitted functions.

V. MEASUREMENTS OF $a_{CP}^{T\text{-odd}}$ IN SUBREGIONS OF PHASE SPACE

The distributions of invariant mass for pairs of final-state particles exhibit significant peaks corresponding to intermediate states $\phi(1020)$, $K^*(892)^{0,+}$, and $\rho(770)$. These states give rise to different strong phases among decay amplitudes, and this can lead to different amounts of direct CP violation. Thus, we search for CP violation in ranges of invariant mass corresponding to a decay proceeding through intermediate resonances ϕ , ρ , or K^* : $|M_{KK} - m_\phi| < 10 \text{ MeV}/c^2$, $-90 \text{ MeV}/c^2 < (M_{\pi^+\pi^0} - m_\rho) < 60 \text{ MeV}/c^2$, and $|M_{K\pi} - m_{K^*}| < 60 \text{ MeV}/c^2$. The requirements for seven different intermediate decays are listed in Table II. We analyze these regions only for SCS and CF decays, as the signal yield for the DCS decay $D^+ \rightarrow K^+ \pi^- \pi^+ \pi^0$ is too low. The subregions of invariant mass correspond to the $D^+ \rightarrow K^\pm h^\mp \pi^+ \pi^0$ decay proceeding via $D^+ \rightarrow \phi \rho^+$, $\bar{K}^{*0} K^{*+}$, and $\bar{K}^{*0} \rho^+$; and the $D_s^+ \rightarrow K^+ h^- \pi^+ \pi^0$ decay proceeding via $D_s^+ \rightarrow K^{*+} \rho^0$, $K^{*0} \rho^+$, $\phi \rho^+$, and $\bar{K}^{*0} K^{*+}$. For the $D_{(s)}^+ \rightarrow \bar{K}^{*0} K^{*+}$ subsamples, we additionally require $|M_{KK} - m_\phi| > 10 \text{ MeV}/c^2$ in order to remove contamination from $D_{(s)}^+ \rightarrow \phi \pi^+ \pi^0$ decays. For this measurement, we use the same fitting procedure as used for the $a_{CP}^{T\text{-odd}}$ measurement over the entire phase space. For each invariant-mass subregion, we first perform an $M(D)$ fit to obtain the shape of signal and background. The floated parameters of the signal PDF (δ_μ and k_σ)

and the background PDF are allowed to differ among different subregions. We subsequently perform a simultaneous fit to the four C_T samples. The resulting values of $a_{CP}^{T\text{-odd}}$ are listed in Table II, and projections of the fits are shown in Fig. 2 for D^+ decays and in Fig. 3 for D_s^+ decays. The subregion dominated by $D_s^+ \rightarrow K^{*0} \rho^+$ has the largest CP asymmetry: $a_{CP}^{T\text{-odd}} = (6.2 \pm 3.0 \pm 0.4)\%$, which differs from zero by 2σ .

VI. SYSTEMATIC UNCERTAINTIES

Many of the systematic uncertainties in the measurements of C_T and \bar{C}_T cancel in the ratios A_T and \bar{A}_T (Eq. 2) or in the difference between them (Eq. 3). The uncertainties that do not cancel are discussed below and listed in Table III. For a given decay mode, the total systematic uncertainty is the sum in quadrature of the individual contributions. For our measurements corresponding to subregions of phase space as listed in Table II, we evaluate systematic uncertainties in an identical manner; these results are listed in Table IV.

(1) C_T -dependent efficiency

We study the dependence of the reconstruction efficiency on C_T using a large sample of MC signal events. We find that events with smaller $|C_T|$ values have lower efficiency due to the fact that the final-state π^0 tends to have lower momentum. To assign a systematic uncertainty for this, we fit the C_T -dependent efficiencies with a polynomial function $\varepsilon(C_T) = \varepsilon_0 + c_1 \cdot |C_T| + c_2 \cdot |C_T|^2$. This fit is performed separately for the $D_{(s)}^+$ subsamples having $C_T > 0$ and $C_T < 0$, and similarly for $D_{(s)}^-$. With these functions, we weight $D_{(s)}^\pm$ candidates in data by the reciprocals of their efficiencies (normalized by the average efficiency) and repeat the fit for $a_{CP}^{T\text{-odd}}$. The difference between the fit result and the nominal result for $a_{CP}^{T\text{-odd}}$, while consistent with zero as expected, is conservatively assigned as a systematic uncertainty due to a possible C_T -dependence of the reconstruction efficiency.

(2) C_T -resolution effects

The resolution in C_T can affect $a_{CP}^{T\text{-odd}}$ if the smearing of events from positive to negative C_T values differs from the smearing of events from negative to positive values. This is studied using a large MC sample to calculate the resolution function for different slices of C_T . A double-Gaussian function is used to model the resolution. The effective width of the double Gaussian is plotted as a function of C_T , and the resulting distribution is fitted to a polynomial $f(x) = a_0 + a_1 x + a_2 x^2$. The fitted value of a_1 ,

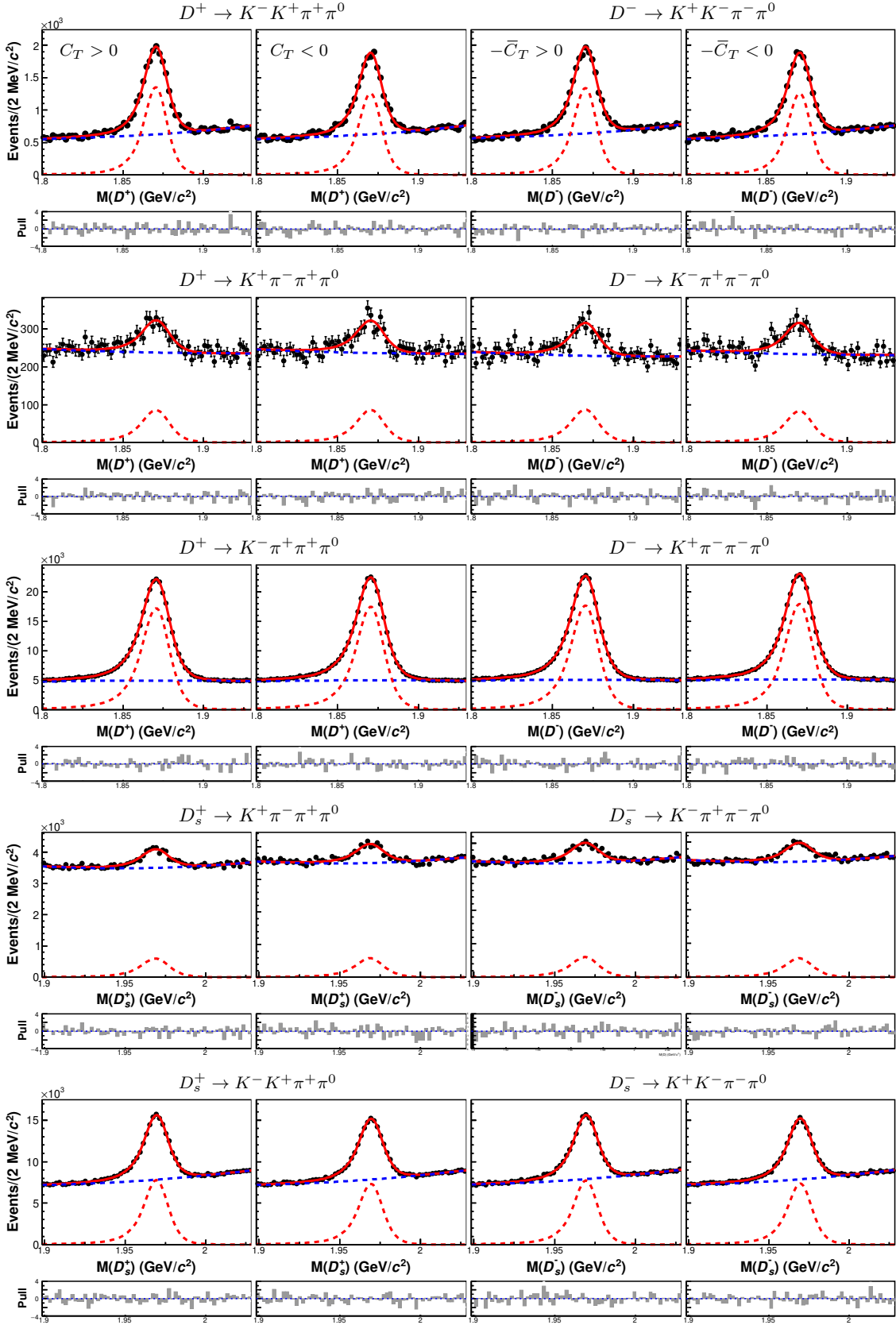


FIG. 1. Mass distributions $M(D_{(s)}^{\pm})$ for signal candidates and the fit results. The rows correspond to the decay modes listed. The columns correspond to the four subsamples $D_{(s)}^+$ with $C_T > 0$, $D_{(s)}^+$ with $C_T < 0$, $D_{(s)}^-$ with $-\bar{C}_T > 0$, and $D_{(s)}^-$ with $-\bar{C}_T < 0$, respectively. The points with error bars show the data; the dashed blue curve shows the fitted background; the dashed red curve shows the fitted signal; and the solid red curve shows the overall fit result. The corresponding pull distributions are shown below, where the pull is defined as $(\text{data} - \text{fit})/(\text{uncertainty in data})$.

TABLE I. Fitted $D_{(s)}^+$ and $D_{(s)}^-$ signal yields (N_D and $N_{\bar{D}}$, respectively), T -odd asymmetry A_T , and T -odd CP -violating asymmetry $a_{CP}^{T\text{-odd}}$, obtained from a simultaneous fit to the four subsamples of each decay mode. The uncertainties listed are statistical only.

Decay	$D^+ \rightarrow f$			$D_s^+ \rightarrow f$	
	Final state (f)	$K^+ K^- \pi^+ \pi^0$	$K^+ \pi^- \pi^+ \pi^0$	$K^+ \pi^- \pi^+ \pi^0$	$K^+ K^- \pi^+ \pi^0$
N_D	27284 ± 254	2062 ± 127	438432 ± 947	15197 ± 484	167357 ± 786
$N_{\bar{D}}$	27177 ± 255	2044 ± 125	450667 ± 961	14945 ± 479	167064 ± 788
A_T (%)	$+3.63 \pm 0.93$	-0.4 ± 6.0	-0.76 ± 0.22	$+1.4 \pm 3.2$	$+2.96 \pm 0.47$
$a_{CP}^{T\text{-odd}}$ (%)	$+0.26 \pm 0.66$	-1.3 ± 4.2	$+0.02 \pm 0.15$	-1.1 ± 2.2	$+0.22 \pm 0.33$

TABLE II. T -odd CP -violating asymmetries ($a_{CP}^{T\text{-odd}}$) in seven subregions of phase space (see text) corresponding to the intermediate $D_{(s)}^+ \rightarrow VV$ processes listed. The uncertainties listed are statistical and systematic, respectively.

Subregion	$D_{(s)}^+ \rightarrow VV$	Signal region (SR)	$a_{CP}^{T\text{-odd}} (\times 10^{-2})$
(1) SCS	$D^+ \rightarrow \phi \rho^+$	ϕ -SR, ρ^+ -SR	$0.85 \pm 0.95 \pm 0.25$
(2) SCS	$D^+ \rightarrow \bar{K}^{*0} K^{*+}$	$K^{*(0,+)}$ -SR, veto ϕ -SR	$0.17 \pm 1.26 \pm 0.13$
(3) CF	$D^+ \rightarrow \bar{K}^{*0} \rho^+$	K^{*0} -SR, ρ^+ -SR	$0.25 \pm 0.25 \pm 0.13$
(4) SCS	$D_s^+ \rightarrow K^{*0} \rho^+$	K^{*0} -SR, ρ^+ -SR	$6.2 \pm 3.0 \pm 0.4$
(5) SCS	$D_s^+ \rightarrow K^{*+} \rho^0$	K^{*+} -SR, ρ^0 -SR	$1.7 \pm 6.1 \pm 1.5$
(6) CF	$D_s^+ \rightarrow \phi \rho^+$	ϕ -SR, ρ^+ -SR	$0.31 \pm 0.40 \pm 0.43$
(7) CF	$D_s^+ \rightarrow \bar{K}^{*0} K^{*+}$	$K^{*(0,+)}$ -SR, veto ϕ -SR	$0.26 \pm 0.76 \pm 0.37$

the coefficient of the asymmetric term, is consistent with zero, and thus the effects of C_T resolution are expected to be small.

To determine the effect on $a_{CP}^{T\text{-odd}}$, we smear the C_T distributions by Gaussian functions having widths given by the previously fitted polynomial $a_0 + a_1 x + a_2 x^2$. We repeat the fit for $a_{CP}^{T\text{-odd}}$ on these smeared samples and take the difference between the resulting value of $a_{CP}^{T\text{-odd}}$ and the nominal value as a systematic uncertainty due to C_T resolution.

(3) Signal and background parameters

We consider systematic uncertainty arising from the fixed parameters of signal and background PDFs as follows. We sample the parameters of the signal PDF from a multi-dimensional Gaussian function, accounting for their respective uncertainties and correlations, and repeat the fit for $a_{CP}^{T\text{-odd}}$. We repeat this procedure 1000 times and take the RMS of the fitted $a_{CP}^{T\text{-odd}}$ values as systematic uncertainties: 0.002% for $D^+ \rightarrow K^- K^+ \pi^+ \pi^0$, 0.023% for $D^+ \rightarrow K^+ \pi^- \pi^+ \pi^0$, 0.004% for $D^+ \rightarrow K^- \pi^+ \pi^+ \pi^0$, 0.054% for $D_s^+ \rightarrow K^+ \pi^- \pi^+ \pi^0$, and 0.003% for $D_s^+ \rightarrow K^- K^+ \pi^+ \pi^0$. We calculate the uncertainty due to fixed values of δ_μ , k_σ , and background parameters in an identical manner; the resulting uncertainties are 0.010%, 0.071%, 0.001%, 0.048%, and 0.002%, respectively. We

sum the two uncertainties in quadrature for each channel to obtain the overall systematic uncertainty due to fixed signal and background parameters.

(4) Signal mass resolution

We consider a possible difference between $D_{(s)}^+$ and $D_{(s)}^-$ samples arising from a difference in mass resolution between data and MC events. To study this effect, we fit the $M(D_{(s)}^+)$ and $M(D_{(s)}^-)$ distributions individually to obtain separate sets of parameters: $(\delta_\mu^+, k_\sigma^+)$ for $D_{(s)}^+$ decays, and $(\delta_\mu^-, k_\sigma^-)$ for $D_{(s)}^-$ decays. With these parameters, we repeat the simultaneous fit to the C_T subsamples. The resulting change in $a_{CP}^{T\text{-odd}}$ is assigned as a systematic uncertainty due to signal mass resolution.

(5) Fit bias

To check for bias in our fitting procedure, we study large samples of ‘‘toy’’ MC events. These events are generated by sampling from the PDFs used to fit the data. We generate 1000 samples each for different input values of $a_{CP}^{T\text{-odd}}$, spanning a range from -0.05 to $+0.05$. We fit these samples and plot the resulting $a_{CP}^{T\text{-odd}}$ values. This distribution is then fitted with a Gaussian function, and the mean and width of the Gaussian are taken as the

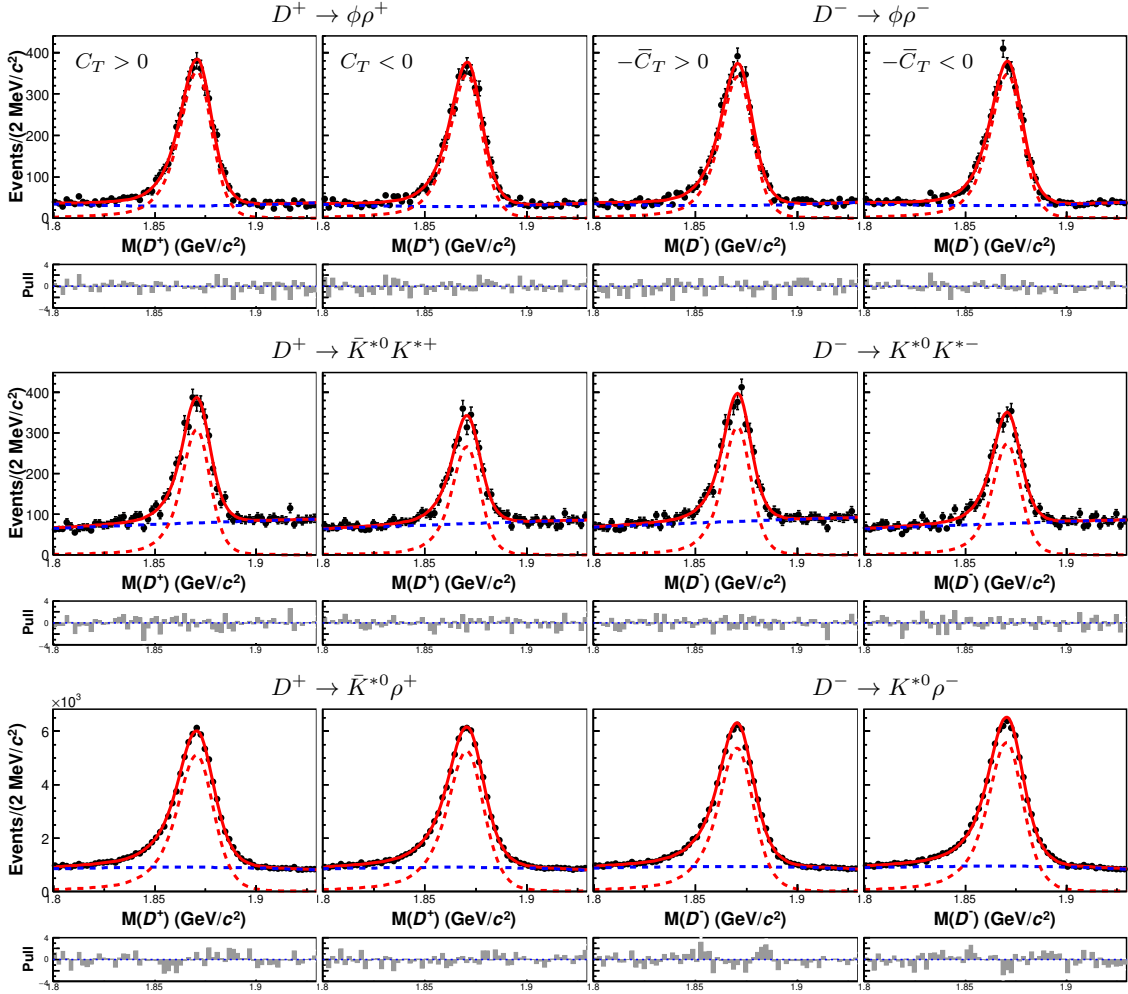


FIG. 2. Mass distributions $M(D^\pm)$ and fit results for subregions of phase space. The rows correspond to the decay modes listed. The columns correspond to the four subsamples D^+ with $C_T > 0$, D^+ with $C_T < 0$, D^- with $-\bar{C}_T > 0$, and D^- with $-\bar{C}_T < 0$, respectively. The points with error bars show the data; the dashed blue curve shows the fitted background; the dashed red curve shows the fitted signal; and the solid red curve shows the overall fit result. The corresponding pull distributions are shown below.

TABLE III. Systematic uncertainties for $a_{CP}^{T\text{-odd}}$ in % for five $D_{(s)}^+$ decay channels: (a) $D^+ \rightarrow K^- K^+ \pi^+ \pi^0$; (b) $D^+ \rightarrow K^+ \pi^- \pi^+ \pi^0$; (c) $D^+ \rightarrow K^- \pi^+ \pi^+ \pi^0$; (d) $D_s^+ \rightarrow K^+ \pi^- \pi^+ \pi^0$; and (e) $D_s^+ \rightarrow K^- K^+ \pi^+ \pi^0$.

Decay channel	(a)	(b)	(c)	(d)	(e)
C_T -dependent efficiency	0.13	0.02	0.08	0.02	0.41
C_T resolution	0.01	0.06	0.01	0.07	0.02
PDF parameters	0.01	0.07	0.01	0.07	0.04
Mass resolution	0.03	0.01	...	0.02	0.11
Fit bias	0.01	0.07	0.00	0.06	0.02
Total syst.	0.13	0.12	0.08	0.12	0.43

mean measured value and its uncertainty corresponding to that input value of $a_{CP}^{T\text{-odd}}$. Plotting these mean values versus the input value displays a linear dependence; fitting a line to these points gives a slope consistent with unity and an intercept consistent with zero. However,

we conservatively assign the difference between our measured value and the input value corresponding to our measured value as given by this fitted line (including its uncertainty) as a systematic uncertainty due to possible fit bias.

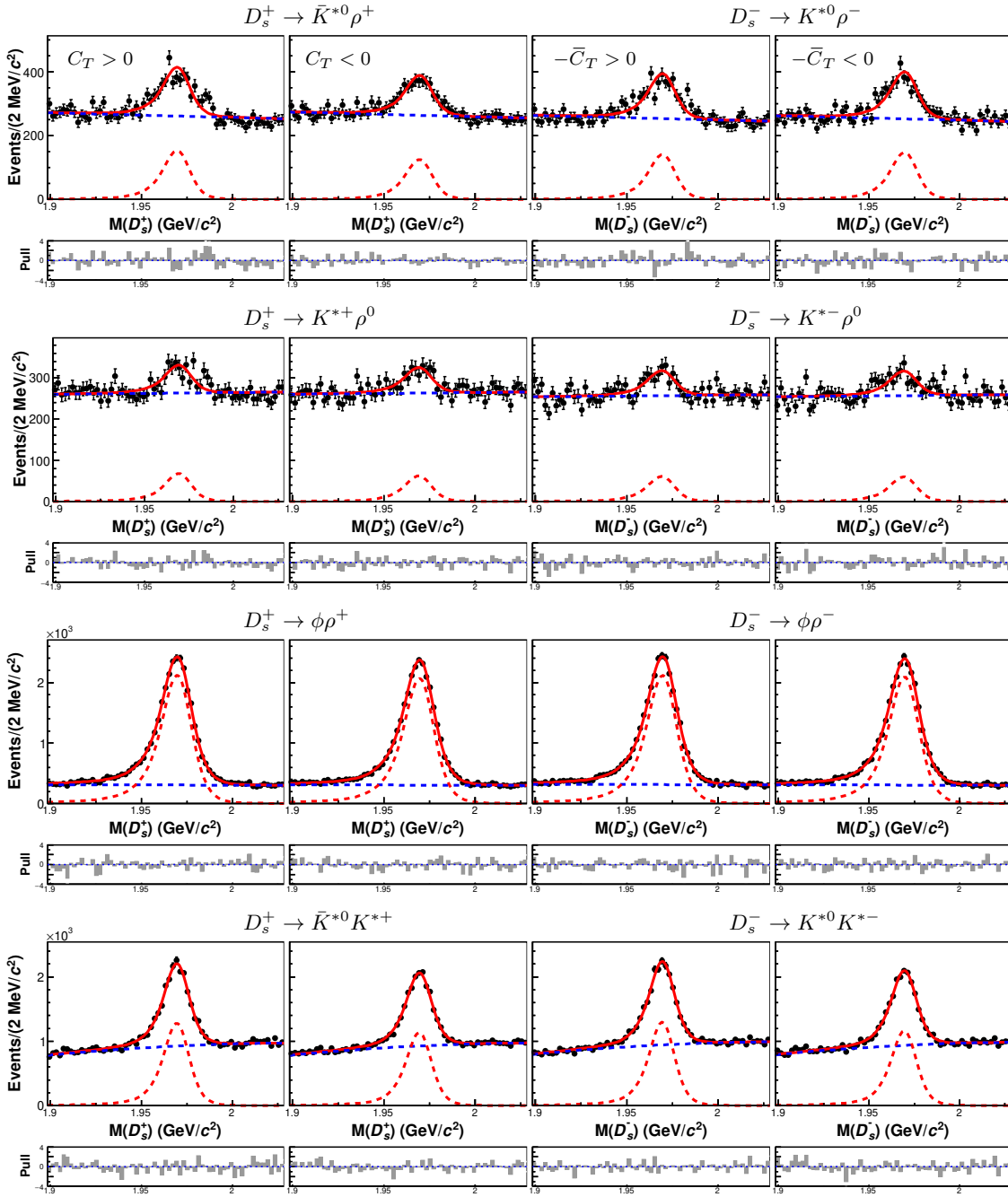


FIG. 3. Mass distributions $M(D_s^\pm)$ and fit results for subregions of phase space. The rows correspond to the decay modes listed. The columns correspond to the four subsamples D_s^+ with $C_T > 0$, D_s^+ with $C_T < 0$, D_s^- with $-\bar{C}_T > 0$, and D_s^- with $-\bar{C}_T < 0$, respectively. The points with error bars show the data; the dashed blue curve shows the fitted background; the dashed red curve shows the fitted signal; and the solid red curve shows the overall fit result. The corresponding pull distributions are shown below.

VII. SUMMARY

We perform a search for CP violation using a T -odd observable for five D_s^\pm decays. Our analysis is based on the full data set of 980 fb^{-1} collected by the Belle experiment. Our results for the CP -violating T -odd parameter

$a_{CP}^{T\text{-odd}}$ are

$$\begin{aligned}
 a_{CP}^{T\text{-odd}}(D^+ \rightarrow K^- K^+ \pi^+ \pi^0) &= (+2.6 \pm 6.6 \pm 1.3) \times 10^{-3} \\
 a_{CP}^{T\text{-odd}}(D^+ \rightarrow K^+ \pi^- \pi^+ \pi^0) &= (-1.3 \pm 4.2 \pm 0.1) \times 10^{-2} \\
 a_{CP}^{T\text{-odd}}(D^+ \rightarrow K^- \pi^+ \pi^+ \pi^0) &= (+0.2 \pm 1.5 \pm 0.8) \times 10^{-3} \\
 a_{CP}^{T\text{-odd}}(D_s^+ \rightarrow K^+ \pi^- \pi^+ \pi^0) &= (-1.1 \pm 2.2 \pm 0.1) \times 10^{-2}
 \end{aligned}$$

TABLE IV. Systematic uncertainties for $a_{CP}^{T\text{-odd}}$ in % for seven subregions of phase space as defined in Table II. These subregions correspond to various two-body intermediate processes.

Source	(1)	(2)	(3)	(4)	(5)	(6)	(7)
C_T -dependent efficiency	0.24	0.13	0.13	0.29	1.17	0.43	0.37
C_T resolution	0.07	0.00	0.00	0.06	0.16	0.05	0.02
PDF parameters	0.01	0.02	0.00	0.09	0.55	0.00	0.01
Mass resolution	0.01	0.02	...	0.26	0.80	0.01	0.01
Fit bias	0.03	0.01	0.01	0.03	0.09	0.00	0.03
Total syst.	0.25	0.13	0.13	0.41	1.53	0.43	0.37

$$a_{CP}^{T\text{-odd}}(D_s^+ \rightarrow K^- K^+ \pi^+ \pi^0) = (+2.2 \pm 3.3 \pm 4.3) \times 10^{-3},$$

ACKNOWLEDGMENTS

where the first uncertainties are statistical and the second uncertainties are systematic. These values are all consistent with zero and show no evidence of CP violation. We plot these values in Fig. 4 along with other measurements of $a_{CP}^{T\text{-odd}}$ in charm meson decays [16, 30, 31]. Our results are the first such measurements for these decay modes and are among the world's most precise measurements for charm decays.

This work, based on data collected using the Belle detector, which was operated until June 2010, was supported by the Ministry of Education, Culture, Sports, Science, and Technology (MEXT) of Japan, the Japan Society for the Promotion of Science (JSPS), and the Tau-Lepton Physics Research Center of Nagoya University; the Australian Research Council including grants DP210101900, DP210102831, DE220100462, LE210100098, LE230100085; Austrian Federal Ministry of Education, Science and Research (FWF) and FWF Austrian Science Fund No. P 31361-N36; National Key R&D Program of China under Contract No. 2022YFA1601903, National Natural Science Foundation of China and research grants No. 11575017, No. 11761141009, No. 11705209, No. 11975076, No. 12135005, No. 12150004, No. 12161141008, and No. 12175041, and Shandong Provincial Natural Science Foundation Project ZR2022JQ02; the Ministry of Education, Youth and Sports of the Czech Republic under Contract No. LTT17020; the Czech Science Foundation Grant No. 22-18469S; Horizon 2020 ERC Advanced Grant No. 884719 and ERC Starting Grant No. 947006 ‘‘InterLeptons’’ (European Union); the Carl Zeiss Foundation, the Deutsche Forschungsgemeinschaft, the Excellence Cluster Universe, and the Volkswagen-Stiftung; the Department of Atomic Energy (Project Identification No. RTI 4002) and the Department of Science and Technology of India; the Istituto Nazionale di Fisica Nucleare of Italy; National Research Foundation (NRF) of Korea Grant Nos. 2016R1D1A1B02012900, 2018R1A2B3003643, 2018R1A6A1A06024970, RS2022-00197659, 2019R1I1A3A01058933, 2021R1A6A1A-03043957, 2021R1F1A1060423, 2021R1F1A1064008, 2022R1A2C1003993; Radiation Science Research Institute, Foreign Large-size Research Facility Application Supporting project, the Global Science Experimental Data Hub Center of the Korea Institute of Science and Technology Information and KREONET/GLORIAD; the Polish Ministry of Science and Higher Education and the National Science Center; the Ministry of Science and Higher Education of the Russian Federation, Agreement

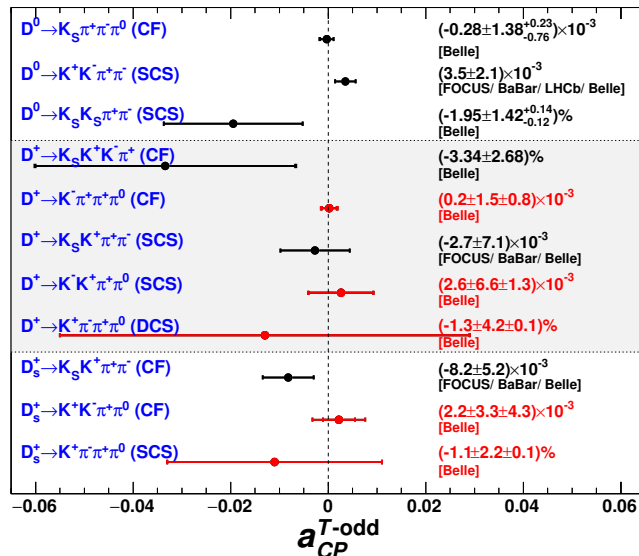


FIG. 4. Our results for $a_{CP}^{T\text{-odd}}$ (in red) along with other measurements of $a_{CP}^{T\text{-odd}}$ for D^0 and D_s^+ decays [16, 30, 31]. For decays in which more than one measurement has been made, the world average value is plotted.

We also measure $a_{CP}^{T\text{-odd}}$ in subregions of phase space corresponding to intermediate processes $D^+ \rightarrow \phi \rho^+$, $\bar{K}^{*0} K^{*+}$, and $\bar{K}^{*0} \rho^+$; and $D_s^+ \rightarrow K^{*+} \rho^0$, $K^{*0} \rho^+$, $\phi \rho^+$, and $\bar{K}^{*0} K^{*+}$. These results, as listed in Tab. II, are also consistent with zero and show no evidence of CP violation.

14.W03.31.0026, and the HSE University Basic Research Program, Moscow; University of Tabuk research grants S-1440-0321, S-0256-1438, and S-0280-1439 (Saudi Arabia); the Slovenian Research Agency Grant Nos. J1-9124 and P1-0135; Ikerbasque, Basque Foundation for Science, Spain; the Swiss National Science Foundation; the Ministry of Education and the Ministry of Science and Technology of Taiwan; and the United States Department of Energy and the National Science Foundation. These acknowledgements are not to be interpreted as an endorsement of any statement made by any of our institutes, funding agencies, governments, or their representatives. We thank the KEKB group for the excellent operation of the accelerator; the KEK cryogenics group for the efficient operation of the solenoid; and the KEK computer group and the Pacific Northwest National Laboratory (PNNL) Environmental Molecular Sciences Laboratory (EMSL) computing group for strong computing support; and the National Institute of Informatics, and Science Information NETWORK 6 (SINET6) for valuable network support.

-
- [1] A. D. Sakharov, *Pisma Zh. Eksp. Teor. Fiz.* **5**, 32 (1967).
 [2] N. Cabibbo, *Phys. Rev. Lett.* **10**, 531 (1963).
 [3] M. Kobayashi and T. Maskawa, *Prog. Theor. Phys.* **49**, 652 (1973).
 [4] J. Brod, A. L. Kagan, and J. Zupan, *Phys. Rev. D* **86**, 014023 (2012).
 [5] H.-n. Li, C.-D. Lu, and F.-S. Yu, *Phys. Rev. D* **86**, 036012 (2012).
 [6] H.-Y. Cheng and C.-W. Chiang, *Phys. Rev. D* **85**, 034036 (2012), [Erratum: *Phys.Rev.D* 85, 079903 (2012)].
 [7] F. Buccella, M. Lusignoli, A. Pugliese, and P. Santorelli, *Phys. Rev. D* **88**, 074011 (2013).
 [8] R. Aaij *et al.* (LHCb Collaboration), *Phys. Rev. Lett.* **122**, 211803 (2019).
 [9] A. Datta and D. London, *Int. J. Mod. Phys. A* **19**, 2505 (2004).
 [10] J. M. Link *et al.* (FOCUS Collaboration), *Phys. Lett. B* **622**, 239 (2005).
 [11] J. P. Lees *et al.* (BABAR Collaboration), *Phys. Rev. D* **84**, 031103 (2011).
 [12] P. del Amo Sanchez *et al.* (BABAR Collaboration), *Phys. Rev. D* **81**, 111103 (2010).
 [13] R. Aaij *et al.* (LHCb Collaboration), *JHEP* **10**, 005.
 [14] K. Prasanth *et al.* (Belle Collaboration), *Phys. Rev. D* **95**, 091101 (2017).
 [15] J. B. Kim *et al.* (Belle Collaboration), *Phys. Rev. D* **99**, 011104 (2019).
 [16] A. Sangal *et al.* (Belle Collaboration), *Phys. Rev. D* **107**, 052001 (2023).
 [17] X.-W. Kang and H.-B. Li, *Phys. Lett. B* **684**, 137 (2010).
 [18] S. Kurokawa and E. Kikutani, *Nucl. Instrum. Meth. A* **499**, 1 (2003), and other papers included in this Volume; T. Abe *et al.*, *Prog. Theor. Exp. Phys.* **2013**, 03A001 (2013) and references therein.
 [19] A. Abashian *et al.* (Belle Collaboration), *Nucl. Instrum. Meth. A* **479**, 117 (2002); also see Section 2 in J. Brodzicka *et al.*, *Prog. Theor. Exp. Phys.* **2012**, 04D001 (2012).
 [20] T. Sjöstrand, P. Edén, C. Friberg, L. Lönnblad, G. Miu, S. Mrenna, and E. Norrbin, *Comput. Phys. Commun.* **135**, 238 (2001).
 [21] D. J. Lange, *Nucl. Instrum. Meth. A* **462**, 152 (2001).
 [22] R. Brun *et al.*, CERN Report No. CERN-DD-EE-84-1 (1987).
 [23] E. Barberio and Z. Wąs, *Comput. Phys. Commun.* **79**, 291 (1994).
 [24] L. K. Li *et al.* (Belle Collaboration), *Phys. Rev. D* **107**, 033003 (2023).
 [25] E. Nakano, *Nucl. Instrum. Meth. A* **494**, 402 (2002).
 [26] K. Hanagaki, H. Kakuno, H. Ikeda, T. Iijima, and T. Tsukamoto, *Nucl. Instrum. Meth. A* **485**, 490 (2002).
 [27] A. Abashian *et al.*, *Nucl. Instrum. Meth. A* **491**, 69 (2002).
 [28] R. L. Workman *et al.* (Particle Data Group), *Prog. Theor. Exp. Phys.* **2022**, 083C01 (2022).
 [29] J. Gaiser *et al.*, *Phys. Rev. D* **34**, 711 (1986).
 [30] Y. S. Amhis *et al.* (HFLAV), *Eur. Phys. J. C* **81**, 226 (2021).
 [31] H. K. Moon *et al.* (Belle Collaboration), (2023), arXiv:2305.11405 [hep-ex].